Archive of Applied Mechanics 74 (2005) 563–579 © Springer-Verlag 2005
DOI 10.1007/s00419-005-0375-8

# A new meshless method for steady-state heat conduction problems in anisotropic and inhomogeneous media

**H. Wang, Q.-H. Qin, Y. L. Kang**



**Summary** A new meshless method is developed to analyze steady-state heat conduction problems with arbitrarily spatially varying thermal conductivity in isotropic and anisotropic materials. The analog equation is used to construct equivalent equations to the original differential equation so that a simpler fundamental solution of the Laplacian operator can be employed to take the place of the fundamental solutions related to the original governing equation. Next, the particular solution is approximated by using radial basis functions, and the corresponding homogeneous solution is solved by means of the virtual boundary collocation method. As a result, a new method fully independent of mesh is developed. Finally, several numerical examples are implemented to demonstrate the efficiency and accuracy of the proposed method. The numerical results show good agreement with the actual results.

**Keywords** Meshless method, Heat conduction, Fundamental solution, Analog equation method, Radial basis function, Isotropic materials, Anisotropic materials

## 1 Introduction

The meshless numerical method has recently become an alternative to the finite element method (FEM) and the boundary element method (BEM) due to its property of avoiding meshing and remeshing, effective treatment of complicated load conditions, and avoidance of mesh distortion in large-deformation problems. The meshless method is usually divided into two main categories: the boundary-type meshless method and the domain-type meshless method. Since the method proposed in this paper belongs to the boundary-type meshless method, developments corresponding to this direction only are briefly reviewed here.

Generally, BEM only involves discretization of the boundary of the structure, due to the governing differential equation being satisfied exactly inside the domain, which leads to a smaller system size with adequate accuracy. This is an important advantage over domain-type solutions such as FEM or the finite difference method (FDM). This advantage exists only for problems without body forces and having explicit fundamental solutions. When a problem involves body forces, a domain discretization is also required, which may cause some inconvenience in the implementation of the BEM. In order to overcome this drawback, Nowak and Brebbia [1, 2] developed a multiple-reciprocity method (MRM), which can convert domain integrals to boundary integrals. Additionally, the dual-reciprocity method (DRM) was introduced by Nardini and Brebbia [3] for transferring domain integrals to boundary integrals. Nowak and Partridge [4] compared these two methods and identified their advantages and drawbacks. The use of the analog equation method [5] makes it possible to treat such problems in which there are no available explicit fundamental solutions. From the discussion above it is evident that the methods mentioned still need to divide a boundary into elements. In order to

*Received 1 November 2004; accepted for publication 26 January 2005*

H. Wang, Q.-H. Qin (✉), Y. L. Kang
Department of Mechanics, Tianjin University, Tianjin, 300072, P.R. China.

Q.-H. Qin
Department of Engineering, Australian National University, Canberra, ACT 0200, Australia. e-mail: qinghua.qin@anu.edu.au

This work was supported by the National Natural Science Foundation of China (No. 10472082) and Australian Research Council.

overcome this disadvantage, many boundary collocation methods have been proposed in the past few decades. Sun et al. [6, 7] proposed a virtual boundary collocation method to avoid the singularity of fundamental solutions, applying this method successfully to solve many engineering problems. In fact, this can be viewed as a kind of method of fundamental solutions (MFS) [8]. However, they did not include a proper process for dealing with body sources. The appearance of radial basis functions (RBFs) provides the possibility of developing a real meshless method. Recently, Chen and Tanaka [9] presented a boundary knot method (BKM) based on the dual-reciprocity principle and the nonsingular general solution. Later, Chen and Hon [10] presented numerical investigations into the convergence of the BKM. In addition, Chen [11, 12] developed the boundary particle method (BPM), based on the multiple-reciprocity principle and the nonsingular general solution, for the analysis of potential problems.



This paper presents a meshless method developed by combining the virtual boundary collocation method (VBCM) [6] with RBF approximation and the analog equation method [5], which can be used to solve isotropic and anisotropic heat conduction problems. RBFs here are used to approximate particular solutions related to a fictitious internal source, which appears when the analog equation method is introduced, and the VBCM is used to compute corresponding homogeneous solutions (see Sect. 3). The analog equation method makes it possible to use a simpler fundamental solution for the Laplacian operator to analyze complicated problems whose fundamental solutions are probably very complicated or difficult to obtain. To verify the performance of the method presented in the paper, several numerical examples are considered (see Sect. 4), and the results show that they agree well with the exact solutions. The proposed method is proven to be suitable and efficient for analyzing heat conduction problems, and is easy to extend to more complex engineering problems such as nonlinear problems and piezoelectric problems.

## 2
## Formulation of steady-state heat conduction

The mathematical model for steady-state heat conduction can be represented by a generalized Poisson's equation. It is well known that the temperature field within a fixed configuration is intrinsically related to a single set of well-posed thermal boundary conditions specified on the entire surface of the domain. As such, let us consider a medium in an open-bounded domain $\Omega \subseteq R^d$, where $d$ is the dimension of domain $\Omega$, and assume that $\Omega$ is bounded by a piecewise-smooth boundary $\Gamma$ which may consist of several segments, each being sufficiently smooth in the Liapunov sense. The spatial coordinate $X \in \Omega \subseteq R^d$ is used to represent the position of a point.

### 2.1
### The governing equation for steady-state heat conduction in isotropic heterogeneous media

Let us consider the general heat conduction problem in isotropic media

$$\nabla \cdot [k(X)\nabla u(X)] + f(X) = k(X)\nabla^2 u + \nabla k(X) \cdot \nabla u(X) + f(X) = 0 \tag{1}$$

satisfying the following boundary conditions:

- Dirichlet boundary condition relating to an unknown temperature field

$$u(X) = \bar{u}(X) \quad X \in \Gamma_1 \tag{2a}$$

- Neumann boundary condition for the boundary heat flux

$$q_n(X) = \bar{q}_n(X) \quad X \in \Gamma_2 \tag{2b}$$

- Convection boundary condition

$$q_n(X) = h_\infty (u - u_\infty) \quad X \in \Gamma_3 \tag{2c}$$

where $\nabla^2$ represents the Laplacian operator, $k(X)$ is the spatially varying thermal conductivity, $u(X)$ is the desired temperature field, and the boundary heat flux arising in the boundary conditions is defined as $q_n = -k\frac{\partial u}{\partial x_i} n_i$; $n_i$ are the components of the unit outward normal vector $\mathbf{n}$ to the boundary $\Gamma$. Here and after, repeated indices imply use of the Einstein summation convention unless otherwise indicated. $f(X)$ denotes the internal heat source; $\bar{u}$ and $\bar{q}_n$ are specified values on the boundary; the constant $h_\infty$ is the convection coefficient and $u_\infty$ is the temperature of the environment. For a well-posed problem, $\Gamma = \Gamma_1 \cup \Gamma_2 \cup \Gamma_3$. It should be mentioned that the convection boundary condition is actually a kind of Robin mixed boundary condition.

Equation (1) can apply to a wide range of engineering problems governed by diffusion processes, including, for instance, groundwater flow. Equation (1) will degenerate into the Poisson equation

$$k\nabla^2 u + f(X) = 0 \tag{3}$$

when thermal conductivity is a constant (independent of spatial variables) within the solution domain.

## 2.2
## The governing equation for steady-state heat conduction in anisotropic media



Unlike isotropic materials, whose thermal conductivity is a scalar function, thermal conductivity in general anisotropic materials is represented by a second-order tensor which contains nine components in three dimensions. Thus, the governing equation in the Cartesian coordinate system is written, in this case, as

$$\nabla \cdot [K(X)\nabla u(X)] + f(X) = \frac{\partial u}{\partial x_j}\frac{\partial k_{ij}}{\partial x_i} + k_{ji}\frac{\partial^2 u}{\partial x_j \partial x_i} + f(X) = 0 \tag{4}$$

with the same boundary conditions as Eqs. (2a)–(2c), where $K$ is the thermal conductivity tensor, whose components should obey Onsagar's reciprocity relation $k_{ij} = k_{ji}$, $u(X)$ is the temperature field, and $f(X)$ denotes the internal heat source. The boundary heat flux $q_n(X)$ here is defined as $q_n = -k_{ij}\frac{\partial u}{\partial x_j}n_i$; $n_i$ are the components of the unit outward normal vector $\mathbf{n}$ to the boundary $\Gamma$.

In particular, we have

$$K = \begin{bmatrix} k_{11} & k_{12} \\ k_{12} & k_{22} \end{bmatrix} \tag{5}$$

for the case of a 2D domain.

Equation (4) can be further written as

$$\begin{aligned} \nabla \cdot [K(X)\nabla u(X)] + f(X) = \frac{\partial u}{\partial x_j}\frac{\partial k_{ij}}{\partial x_i} + k_{ji}\frac{\partial^2 u}{\partial x_j \partial x_i} + f(X) = \left(\frac{\partial k_{11}}{\partial x_1} + \frac{\partial k_{12}}{\partial x_2}\right)\frac{\partial u}{\partial x_1} + \left(\frac{\partial k_{12}}{\partial x_1} + \frac{\partial k_{22}}{\partial x_2}\right)\frac{\partial u}{\partial x_2} \\ + 2k_{12}\frac{\partial^2 u}{\partial x_1 \partial x_2} + k_{11}\frac{\partial^2 u}{\partial x_1^2} + k_{22}\frac{\partial^2 u}{\partial x_2^2} + f(X) = 0 \end{aligned} \tag{6}$$

If the coefficients $k_{ij}$ are assumed to be independent of the space variables, Eq. (6) can be simplified as

$$\nabla \cdot [K(X)\nabla u(X)] + f(X) = k_{11}\frac{\partial^2 u}{\partial x_1^2} + k_{22}\frac{\partial^2 u}{\partial x_2^2} + 2k_{12}\frac{\partial^2 u}{\partial x_1 \partial x_2} + f(X) = 0 \tag{7}$$

In heat conduction, the most significant quantity to characterize the anisotropy of a medium is the determinant of the thermal conductivity matrix, which takes the form $|k_{ij}| = k_{11}k_{22} - k_{12}^2$ for 2D heat conduction. The smaller the value of $|k_{ij}|$, the more asymmetric the temperature fields and the behavior of the heat flux vectors. Since the criterion $|k_{ij}| > 0$ determines the type of differential equation (parabolic for transient problems and elliptic for steady problems), the smaller the value of $|k_{ij}|$ is, the more difficult the numerical calculation will be, see Chang et al. [13].

## 3
## Implementation of the proposed meshless method

Since the problem to be studied is linear, a general linear differential operator $L$ is introduced for the sake of convenience. Thus, Eqs. (1) and (4) can be replaced by

$$L\,[u(X)] + f(X) = 0 \tag{8}$$

where

$$L = k\nabla^2 + \nabla k \cdot \nabla \tag{9}$$

for isotropic materials and

$$L = \frac{\partial}{\partial x_j}\frac{\partial k_{ij}}{\partial x_i} + k_{ji}\frac{\partial^2}{\partial x_i \partial x_j} \tag{10}$$

for anisotropic materials.

### 3.1
### The analog equation method

The boundary value problems (BVPs) described by Eqs. (8) and (2a)–(2c) can be converted into a Poisson-type equation using the analog equation method [5]. For this purpose, suppose $u(X)$ is the sought solution to the BVPs, which is a continuously differentiable function with up to two orders in $\Omega$. If the Laplacian operator is applied to this function, namely,



$$\nabla^2 u = b(X) \tag{11}$$

then, Eq. (11) indicates that the solution of Eq. (8) can be established by solving this linear equation under the same boundary conditions (2a)–(2c), if the fictitious source distribution $b(X)$ is known. The solution procedure is detailed here.

Since this is a linear problem, the solution to Eq. (6) can be written as a sum of the homogeneous solution $u^{\text{hom}}$ and the inhomogeneous, or particular, solution $u^{\text{par}}$, that is

$$u = u^{\text{hom}} + u^{\text{par}} \tag{12}$$

Accordingly, $u^{\text{hom}}$ and $u^{\text{par}}$ should, respectively, satisfy

$$\nabla^2 u^{\text{par}}(X) = b(X) \tag{13}$$

and

$$\begin{cases} \nabla^2 u^{\text{hom}}(X) = 0 & X \in \Omega \\ u^{\text{hom}}(X) = \bar{u} - u^{\text{par}}(X) & X \in \Gamma_1 \\ q_n^{\text{hom}}(X) = \bar{q}_n - q_n^{\text{par}}(X) & X \in \Gamma_2 \\ h_\infty u^{\text{hom}}(X) - q_n^{\text{hom}}(X) = h_\infty u_\infty - h_\infty u^{\text{par}} + q_n^{\text{par}} & X \in \Gamma_3 \end{cases} \tag{14}$$

### 3.2
### The RBF approximation for the particular solution

The next step of the proposed approach is to evaluate the particular solution by RBF approximation. To this end, the right-hand side of Eq. (13) can be approximated by

$$b(X) = \sum_{j=1}^{I+B} \alpha_j f_j(X) \tag{15}$$

where $I$ and $B$ are the number of interpolation points inside the domain and on the boundary, respectively, as shown in Fig. 1. $\alpha_j$ are coefficients to be determined, and $f_j$ are a set of approximating functions.

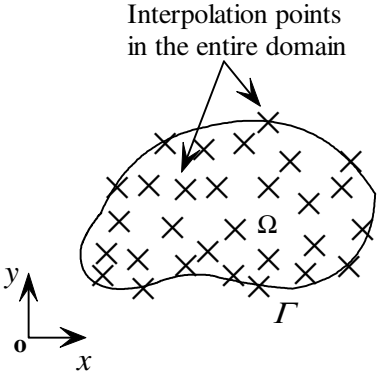


**Fig. 1.** Interpolation points inside the domain and on its boundary

Similarly, the particular solution $u^{\text{par}}$ is also approximated

$$u^{\text{par}}(X) = \sum_{j=1}^{I+B} \alpha_j \hat{u}_j(X) \tag{16}$$

where $\hat{u}_j$ are a corresponding set of particular solutions.

Correspondingly, the boundary heat flux can be expressed as

$$q_n^{\text{par}}(X) = -k \frac{\partial u^{\text{par}}}{\partial x_m} n_m = -k \left[ \sum_{j=1}^{I+B} \alpha_j \frac{\partial \hat{u}_j}{\partial x_m} \right] n_m \tag{17a}$$

for isotropic materials and

$$q_n^{\text{par}}(X) = -k_{mn} \frac{\partial u^{\text{par}}}{\partial x_n} n_m = -k_{mn} \left[ \sum_{j=1}^{I+B} \alpha_j \frac{\partial \hat{u}_j}{\partial x_n} \right] n_m \tag{17b}$$

for anisotropic materials.

Because the particular solutions $u^{\text{par}}$ satisfy Eq. (13), the key to this approximation is the assumption of a corresponding set of approximating particular solutions $\hat{u}_j$, which, for the case of the Laplacian operator, satisfy

$$\nabla^2 \hat{u}_j(X) = f_j(X) \tag{18}$$

The effectiveness and accuracy of the interpolation depends on the choice of the approximating functions $f_j$. Global interpolation functions, such as Lagrange polynomials, Fourier sine and cosine series, or locally distributed functions, such as polynomial-type RBFs and thin plate splines (TPS) may be used [14–16] for this purpose. In this paper, the functions $f_j$ in Eq. (15) are selected to be local RBFs in terms of a power series of a distance function $r_j$. Because even powers of $r_j$ are not RBFs [17], and artificially created singularities may be encountered in some cases [15], the local RBFs can be taken as:

$$f_j(X) = 1 + r_j^3 \tag{19}$$

where $r(X, X_j) = r_j(X) = |X - X_j|$ denotes the distance from the source point $X_j$ to the field point $X$. These functions in Eq. (19) have been found to be most convenient to implement into standard computer programs.

Using Eqs. (18) and (19), the approximating particular solutions $\hat{u}_j$ can be written as

$$\hat{u}_j = \frac{r_j^2}{4} + \frac{r_j^5}{25} \tag{20}$$

for a 2D problem, and

$$\hat{u}_j = \frac{r_j^2}{6} + \frac{r_j^5}{30} \tag{21}$$

for a 3D problem. Since the inhomogeneous term $b(X)$ is an unknown function that depends on the unknown function $u(X)$, the coefficients $\alpha_j$ cannot be determined directly through solution of Eq. (15). However, this problem can be tackled in the following way.

### 3.3
### The virtual boundary collocation method for the homogeneous solution

To obtain a weak solution of the Laplace problem (14), $N$ nodal points $X_j (j = 1, 2, \cdots, N)$ on the real boundary and $N$ fictitious source points $X_i' (i = 1, 2, \cdots N)$ on the virtual boundary are selected, respectively (see Fig. 2). Moreover, assume that, at each fictitious source point, there is a virtual source load $\varphi_i (1 \le i \le N)$.

According to the superposition principle, the potential $u^{\text{hom}}$ and the boundary heat flux at field points $X$ in the domain or on the boundary can be expressed by a linear combination of

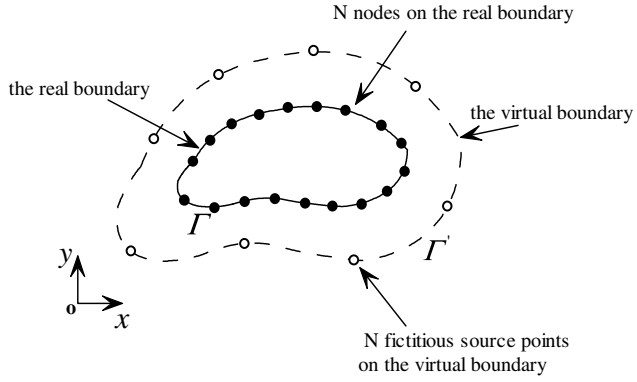


**Fig. 2.** An illustration of a computational domain and points discretized on the real and virtual boundaries

fundamental solutions in terms of fictitious sources located on the virtual boundary, respectively [6, 8], that is

$$u^{\text{hom}}(X) = \sum_{i=1}^{N} u^*(X, X_i')\varphi_i \tag{22}$$

$$q_n^{\text{hom}}(X) = -k\frac{\partial u^{\text{hom}}}{\partial x_m} n_m = -k\left[\sum_{i=1}^{N} \varphi_i \frac{\partial u^*(X, X_i')}{\partial x_m}\right] n_m \tag{23a}$$

for isotropic materials and

$$q_n^{\text{hom}}(X) = -k_{mn}\frac{\partial u^{\text{hom}}}{\partial x_n} n_m = -k_{mn}\left[\sum_{i=1}^{N} \varphi_i \frac{\partial u^*(X, X_i')}{\partial x_n}\right] n_m \tag{23b}$$

for anisotropic materials. $u^*$ is the fundamental solution of the Laplacian operator,

$$u^*(X, Y) = \frac{1}{2\pi} \ln \frac{1}{r(X, Y)} \tag{24}$$

for a 2D problem, and

$$u^*(X, Y) = \frac{1}{4\pi r} \tag{25}$$

for a 3D problem.

It should be pointed out that the number of virtual or fictitious source points is chosen to be equal to the number of nodes on the real boundary in the proposed meshless method. This choice is made for computing convenience. A proper number of these points exists, which can reflect all boundary conditions and requires the minimum possible computing time.

The distance between the fictitious source points and real boundary is another interesting issue. In order to determine the proper location of the virtual boundary, a similarity ratio between the virtual and real boundary is introduced [6] and defined as

$$\text{similarity ratio} = \frac{\text{characteristic length of the virtual boundary}}{\text{characteristic length of the real boundary}}$$

From the point of view of computation, accuracy will decrease if the distance becomes very small, in which case the similarity ratio is close to one, and problems may be caused due to the singularity of the fundamental solutions. Conversely, round-off errors in C/Fortran floating-point arithmetic may be a serious problem when the source points are far from the real boundary. In that case, the coefficient matrix of the system of equations is nearly zero [6, 18]. Therefore, the similarity ratio is generally selected to be in the range of 1.8–4.0 for internal problems and 0.6–0.8 for external problems in practical computation [6].

### 3.4
### The construction of solving equations

According to the above analysis, the solution $u = u(X)$ that we are seeking for Eqs. (8) and (2a)–(2c) can be obtained as

$$u = \sum_{i=1}^{N} \varphi_i u*(X, X_i') + \sum_{j=1}^{I+B} \alpha_j \hat{u}_j \tag{26}$$

$$q_n = -k \left[ \sum_{i=1}^{N} \varphi_i \frac{\partial u^*(X, X_i')}{\partial x_m} + \sum_{j=1}^{I+B} \alpha_j \frac{\partial \hat{u}_j}{\partial x_m} \right] n_m \tag{27a}$$



for isotropic materials and

$$q_n = -k_{mn} \left[ \sum_{i=1}^{N} \varphi_i \frac{\partial u^*(X, X_i')}{\partial x_n} + \sum_{j=1}^{I+B} \alpha_j \frac{\partial \hat{u}_j}{\partial x_n} \right] n_m \tag{27b}$$

for anisotropic materials.

Differentiating Eq. (26) yields

$$\frac{\partial u}{\partial x_m} = \sum_{i=1}^{N} \varphi_i \frac{\partial u^*(X, X_i')}{\partial x_m} + \sum_{j=1}^{I+B} \alpha_j \frac{\partial \hat{u}_j}{\partial x_m} \tag{28a}$$

$$\frac{\partial^2 u}{\partial x_m \partial x_n} = \sum_{i=1}^{N} \varphi_i \frac{\partial u^*(X, X_i')}{\partial x_m \partial x_n} + \sum_{j=1}^{I+B} \alpha_j \frac{\partial \hat{u}_j}{\partial x_m \partial x_n} \tag{28b}$$

Finally, in order to determine the unknowns $\alpha_j$ and $\varphi_i$, Eqs. (26) and (28) should satisfy the governing equation (8) at $I+B$ interpolation points inside $\Omega$ and on its boundary. In addition, Eqs. (26) and (27) should satisfy corresponding boundary conditions (2a)–(2c) at $N$ nodal points on the real boundary. As a result, a system of $N+I+B$ linear equations can be constructed as

$$\begin{cases} \sum_{i=1}^{N} \varphi_i \left[ k\nabla^2 u^* + \nabla k \cdot \nabla u^* \right] + \sum_{j=1}^{I+B} \alpha_j \left[ k\nabla^2 \hat{u}_j + \nabla k \cdot \nabla \hat{u}_j \right] = -f(X) \\ \sum_{i=1}^{N} \varphi_i u^* + \sum_{j=1}^{I+B} \alpha_j \hat{u}_j = \bar{u} \\ \sum_{i=1}^{N} \varphi_i \left( -k \frac{\partial u^*}{\partial x_m} n_m \right) + \sum_{j=1}^{I+B} \alpha_j \left( -k \frac{\partial \hat{u}_j}{\partial x_m} n_m \right) = \bar{q}_n \\ \sum_{i=1}^{N} \varphi_i \left( h_\infty u^* + k \frac{\partial u^*}{\partial x_m} n_m \right) + \sum_{j=1}^{I+B} \alpha_j \left( h_\infty \hat{u}_j + k \frac{\partial \hat{u}_j}{\partial x_m} n_m \right) = h_\infty u_\infty \end{cases} \tag{29}$$

for isotropic materials and

$$\begin{cases} \sum_{i=1}^{N} \varphi_i \left( \frac{\partial u^*}{\partial x_n} \frac{\partial k_{mn}}{\partial x_m} + k_{mn} \frac{\partial^2 u^*}{\partial x_m \partial x_n} \right) + \sum_{j=1}^{I+B} \alpha_j \left( \frac{\partial \hat{u}_j}{\partial x_n} \frac{\partial k_{mn}}{\partial x_m} + k_{mn} \frac{\partial^2 \hat{u}_j}{\partial x_m \partial x_n} \right) = -f(X) \\ \sum_{i=1}^{N} \varphi_i u^* + \sum_{j=1}^{I+B} \alpha_j \hat{u}_j = \bar{u} \\ \sum_{i=1}^{N} \varphi_i \left( -k_{mn} \frac{\partial u^*}{\partial x_n} n_m \right) + \sum_{j=1}^{I+B} \alpha_j \left( -k_{mn} \frac{\partial \hat{u}_j}{\partial x_n} n_m \right) = \bar{q}_n \\ \sum_{i=1}^{N} \varphi_i \left( h_\infty u^* + k_{mn} \frac{\partial u^*}{\partial x_n} n_m \right) + \sum_{j=1}^{I+B} \alpha_j \left( h_\infty \hat{u}_j + k_{mn} \frac{\partial \hat{u}_j}{\partial x_n} n_m \right) = h_\infty u_\infty \end{cases} \tag{30}$$

for anisotropic materials, from which the unknown coefficients $\alpha_j$ and $\varphi_i$ can be determined.

Once these unknown coefficients are determined, the solution $u$ and heat flux at any field point $X$ inside the domain or on its boundary can be calculated using Eqs. (26) and (27).

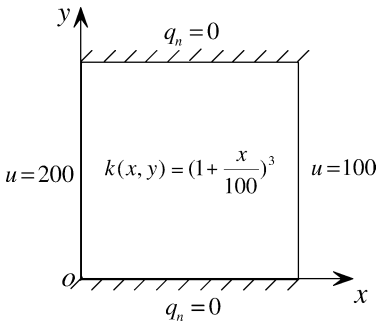


**Fig. 3.** Geometry of square region and boundary conditions



## 4
## Numerical implementation

In order to demonstrate the efficiency and accuracy of the proposed method, several benchmark numerical examples [19–21] are considered and their results are compared with the analytical results.

*Example 1.* As the first example, let us consider a $100 \times 100$ m isotropic square region illustrated in Fig. 3. The top and bottom boundaries are insulated. The left wall is assigned a temperature of 200°C and the right wall is assigned a temperature of 100°C.

The spatial variation of the thermal conductivity is taken to be cubic in the $x$-direction as

$$k(x, y) = \left(1 + \frac{x}{100}\right)^3$$

The problem is two dimensional, and an exact solution is readily given as

$$u(x, y) = \frac{800}{6}\left[\frac{1}{\left(1 + \frac{x}{100}\right)^2} + \frac{1}{2}\right]$$

To compare the different situations more clearly, we need a measurement to judge the overall performance of each situation. Therefore, we define the maximum of the percentage relative error between two functions $f$ and $g$, which represent the exact and numerical solutions, respectively, as

$$\text{maximum of relative error } \% = \max_{(x,y)\in\Omega}\left|\frac{f - g}{f}\right| \times 100\%$$

where $\Omega$ is the domain within which both functions are defined. It is evident that the smaller the maximum relative error, the better an approach.

In this example, Figs. 4 and 5 depict the profile of interpolation points in the square and the virtual boundary, respectively. Different situations are analysed to demonstrate the accuracy and efficiency of the proposed method.

Figure 6 shows the variation of the maximum of percent relative error in temperature within the square domain when the number of interpolation points varies from 20 to 160 and the similarity ratio is 3.0, from which we can see that the greater the number of interpolation points, the smaller the maximum relative error.

Figure 7 depicts the variation of the maximum percentage relative error in temperature within the square domain when the similarity ratio between the virtual and the real boundary varies

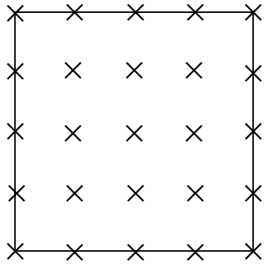

**Fig. 4.** Profile of interpolation points in the square

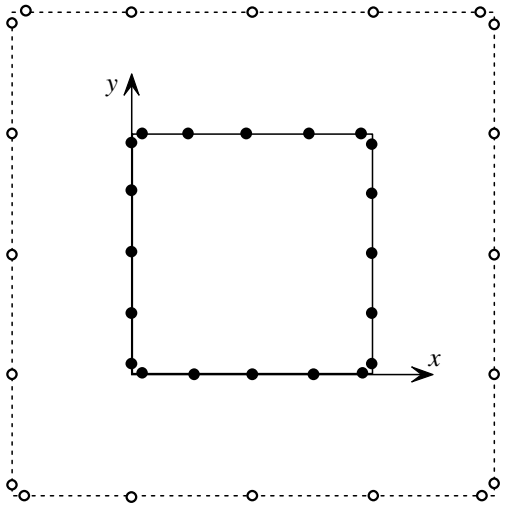


**Fig. 5.** Profile of collocation points on the real and virtual boundaries

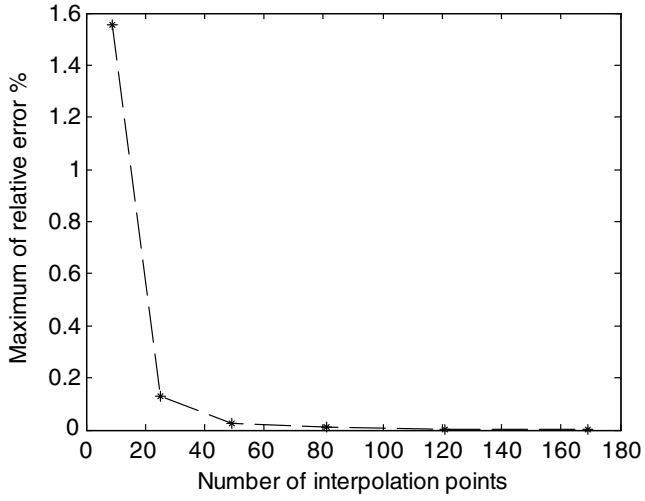


**Fig. 6.** Variation of maximum relative error in temperature in the square when the number of interpolation points varies from 20 to 160 and the similarity ratio is 3.0

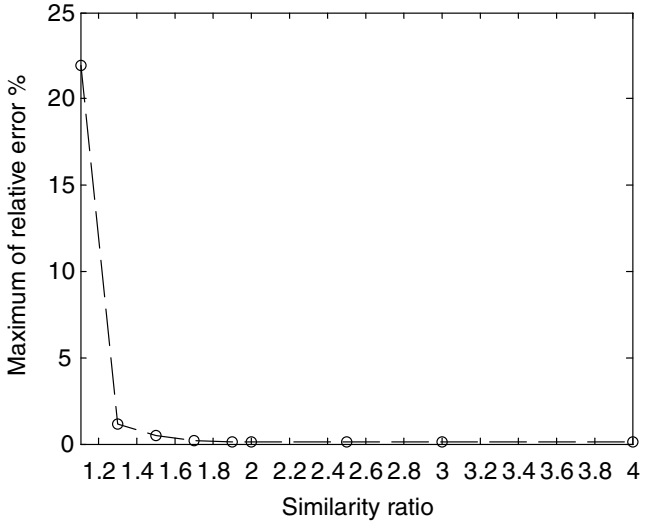


**Fig. 7.** Variation of maximum of relative error in temperature in the square when the similarity ratio varies from 1.8 to 4, while $N = 20$ and $I + B = 25$

from 1.8 to 4, while $N = 20$ and $I + B = 25$. Due to the singularity of the fundamental solutions, accuracy will decrease when the similarity ratio approaches 1, as can be seen from Fig. 7. We also can see that the similarity ratio can be varied within a certain range to obtain stable computing accuracy. Generally, the similarity ratio can be selected in the range of 1.8–4.0.

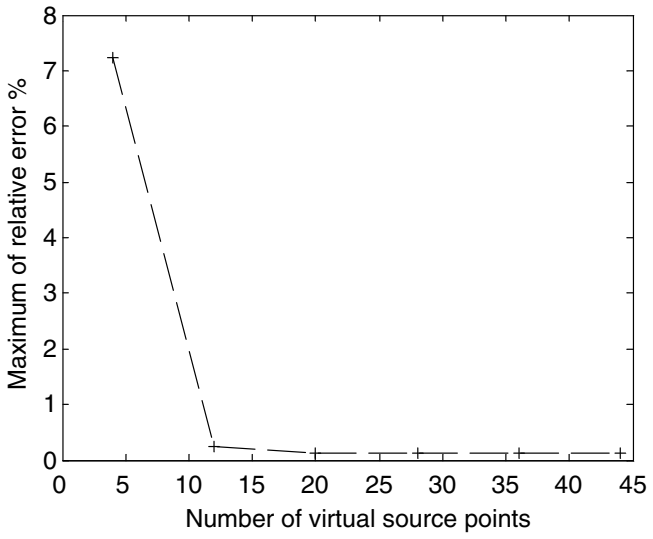


**Fig. 8.** Variation of maximum of relative error in temperature in the square when the number of virtual source points varies from 5 to 45, while $I+B=25$ and the similarity ratio is 3.0

Figure 8 shows the variation of the maximum of percent relative error in temperature within the square domain when the number of fictitious source points outside the domain varies from 5 to 45 with $I+B=25$ and the similarity ratio is 3.0. In this case, no increase in accuracy is evident when the number of virtual source points exceeds 20. The reasons for this effect are the simple boundary and the number of interpolation points.

*Example 2.* Consider an isotropic disc whose radius is 0.1 m. Here, the thermal conductivity is assumed to vary bi-quadratically as

$$k(x,y)=(2x+y+2)^2$$

An analytical expression for the temperature field satisfying the governing heat conduction equation can be given as

$$u(x,y)=\frac{6x^2-6y^2+20xy+30}{2x+y+2}$$

This temperature profile is also used to impose the boundary conditions shown in Fig. 9.

This nonhomogeneous problem is solved using 36 fictitious source points outside the domain (shown in Fig. 10) and 181 interpolation points (shown in Fig. 11). The similarity ratio is 3.0. The distribution of temperature on the boundary of the circle inside the disc is plotted in Fig. 12, while the boundary heat fluxes are plotted in Fig. 13. It is clear from these figures that good agreement is achieved with relatively few collocation points.

*Example 3.* In order to illustrate typical numerical results, we consider a 2D anisotropic medium with a thermal conductivity tensor given by

$$k_{11}=5.0,\quad k_{22}=1.0,\quad k_{12}=k_{21}=2.0$$

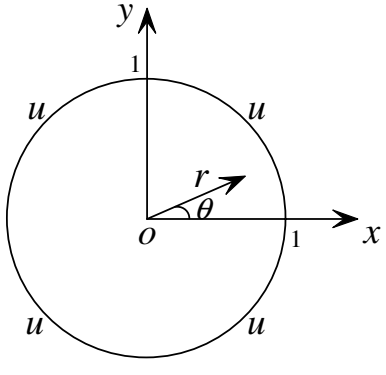


**Fig. 9.** Geometry of the domain and boundary conditions for Example 2

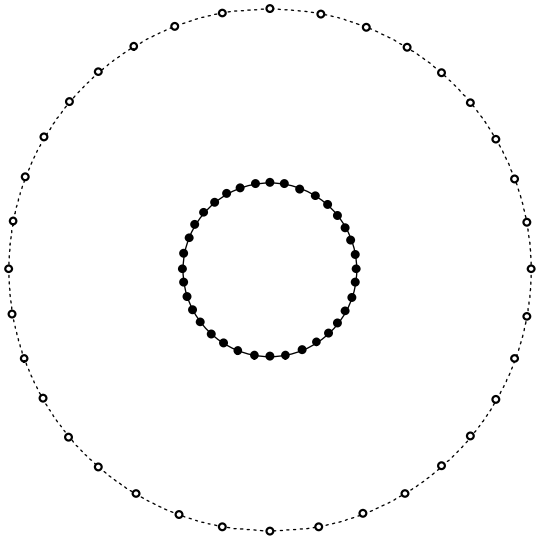

**Fig. 10.** Illustration of collocation points on the virtual and real boundaries in Example 2

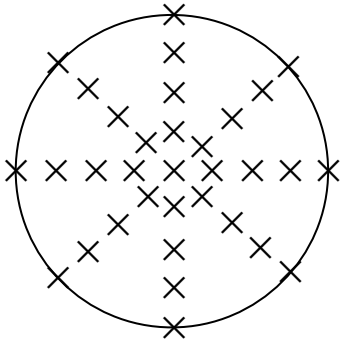

**Fig. 11.** Illustration of interpolation points within the circular domain in Example 2

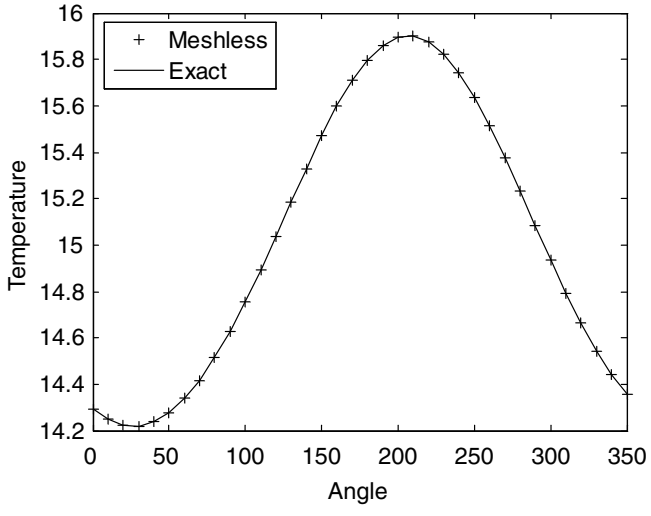


**Fig. 12.** Distribution of temperature on the boundary of inner circle (radius = 0.05 m) inside a disc

The Dirichlet problems are solved in the plane domain $\Omega = \{(x, y) : x^2 + y^2 < 1\}$, i.e. the 2D disc of radius unity. The analytical temperature distribution to be retrieved is given by

$$u(x, y) = \frac{x^3}{5} - x^2 y + xy^2 + \frac{y^3}{5}$$

which imposes the boundary conditions.

In computation, the similarity ratio is selected to be 3.0. The number of fictitious source points on the virtual boundary is 36 and there are 33 interpolation points to be used during the

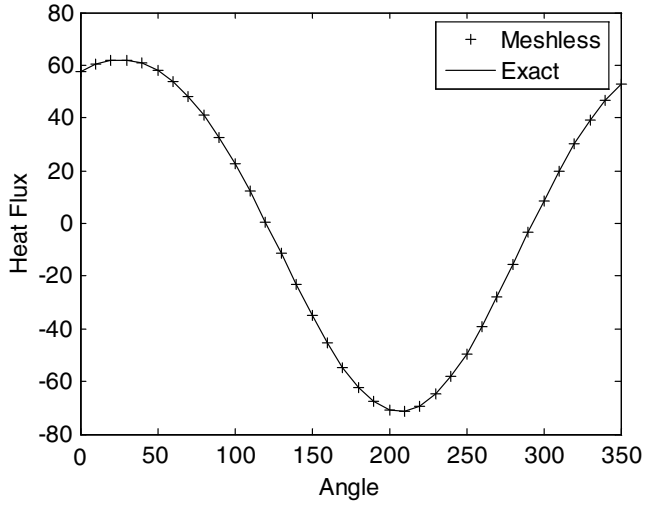


**Fig. 13.** Distribution of heat fluxes on the outer boundary of the disc

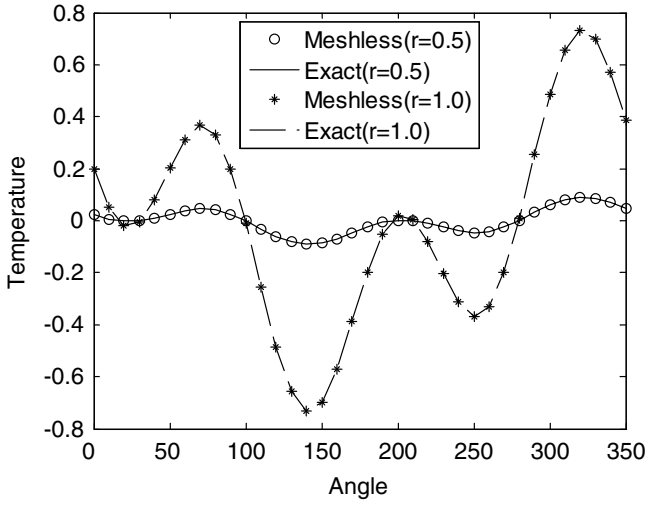


**Fig. 14.** Distribution of temperature on the boundary of circles (radius = 0.5 and 1.0) within a disc

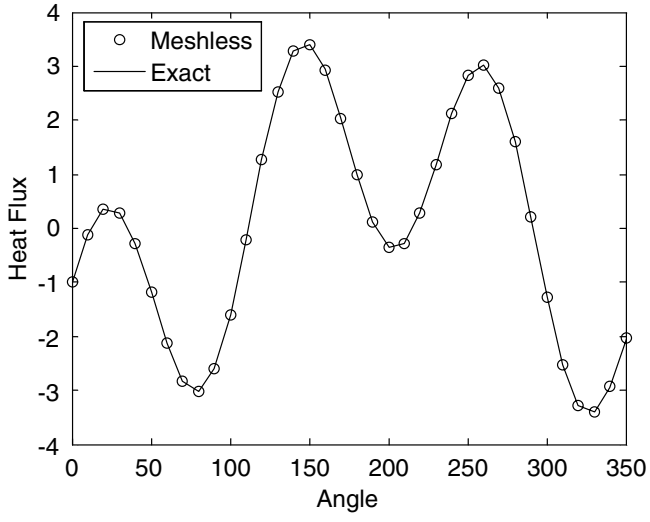


**Fig. 15.** Distribution of heat flux on the boundary of a disc

RBF approximation, including 25 internal points and 8 boundary points. Figure 14 shows the distribution of temperature at the points on the circles whose radii are equal to 0.5 and 1.0, respectively. We can see that good agreement is obtained between the numerical results and the exact solutions.

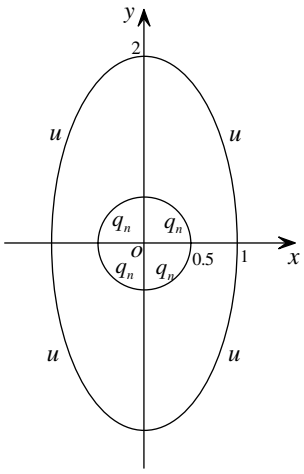


**Fig. 16.** Hollow ellipse and imposed boundary conditions for anisotropic materials

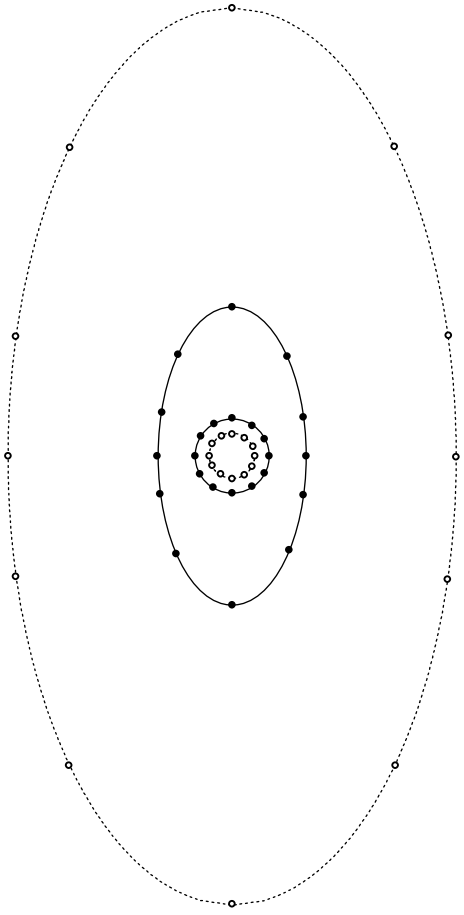

**Fig. 17.** Illustration of collocation points on the virtual and real boundaries

Figure 15 depicts the distribution of heat flux on the boundary and we can see that the numerical results also agree well with the exact results.

*Example 4.* As the latest example, let us consider an orthotropic material in a hollow ellipse whose center is at (0, 0), with the major axis of 2 m in the $y$-direction and the minor axis of 1 m in the $x$-direction. The ellipse then encloses a circle of radius 0.5 m whose center is also at (0, 0). The thermal conductivity is

$$k(x,y)=\begin{bmatrix} 2x+y+5 & 0 \\ 0 & 3x+y+7 \end{bmatrix}$$

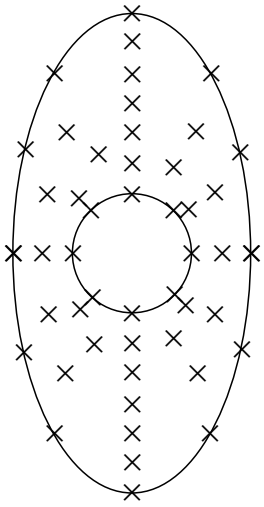

**Fig. 18.** Illustration of interpolation points on the boundary and within the domain

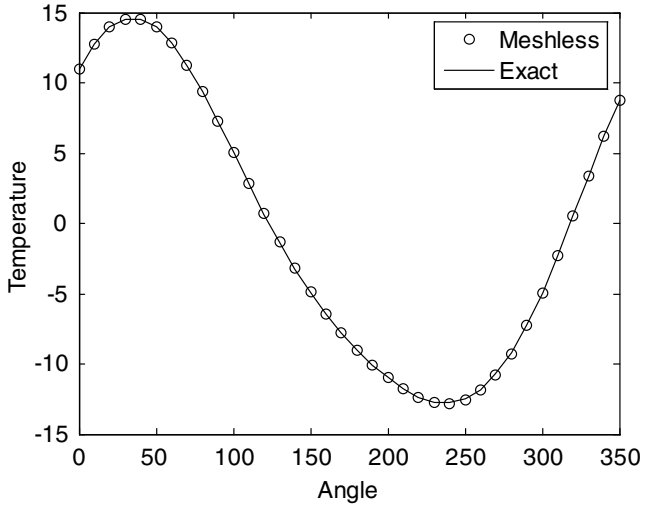


**Fig. 19.** Comparison of temperature between numerical and exact results on the inner circular boundary

The following temperature distribution

$$u(x, y) = 4x^2 + 10xy - 7y^2 + 20x + 18y$$

can be shown to satisfy the governing heat conduction equation with the conductivity given above. As such, it is used to impose the boundary conditions illustrated in Fig. 16.

In computation, 24 fictitious source points on the virtual boundary and the same number of collocation points on the real boundary are employed. The similarity ratios are equal to 3.0 and 0.6, respectively (see Fig. 17). Additionally, 108 internal points and 72 boundary points are selected to form the RBF approximation (see Fig. 18).

The numerical results of temperature and heat flux on the outer elliptic boundary and inner circular boundary are shown in Figs. 19–22 and comparison is made with the analytical results, from which it can be seen that the proposed meshless method achieves high accuracy.

In addition to the results at points on the inner and outer boundaries, the distribution of temperature at some internal points located on the ellipse, which has a semimajor axis of length 1.25 and a semiminor axis of length 0.75, is also computed and presented in Fig. 23. It can be seen again from Fig. 23 that the proposed method has relatively high accuracy.

## 5
## Conclusion

In this paper, a meshless method is developed to solve isotropic and anisotropic heat conduction problems. This is accomplished by combining the VBCM with the concept of analog equation

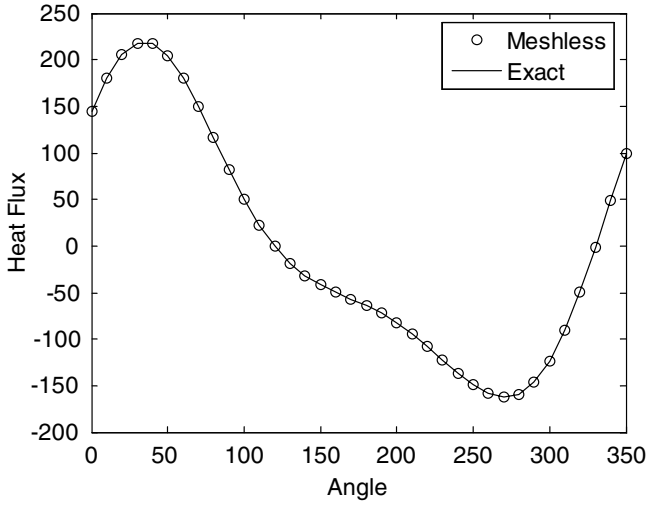


**Fig. 20.** Comparison of heat flux between numerical and exact results on the inner circular boundary

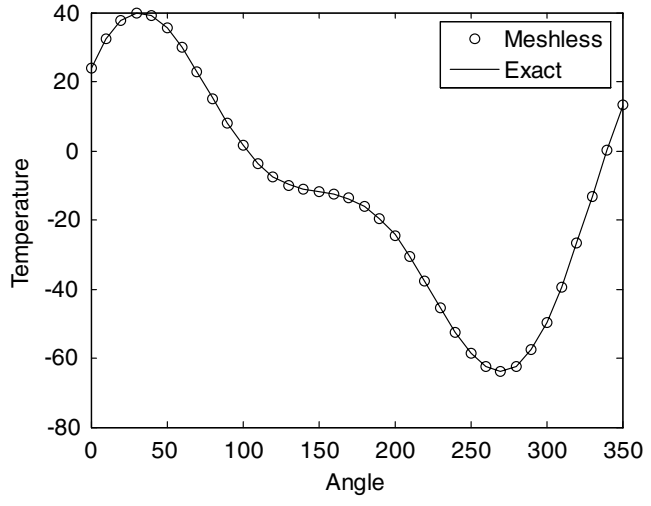


**Fig. 21.** Comparison of temperature between numerical and exact results on the external elliptic boundary

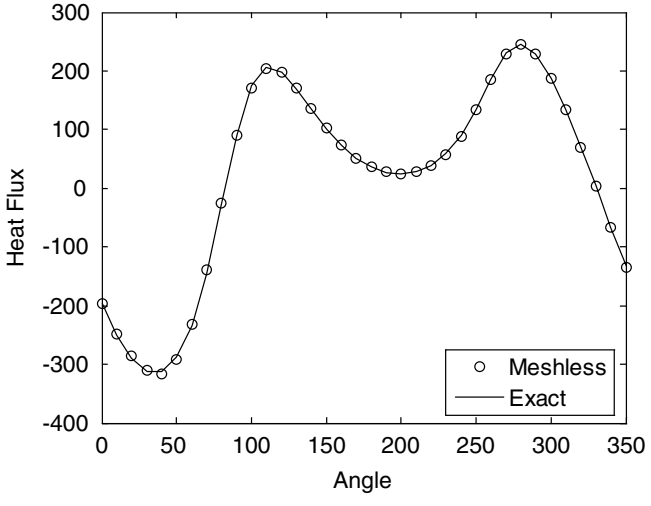


**Fig. 22.** Comparison of heat flux between numerical and exact results on the external elliptic boundary

method and RBF approximation. The proposed meshless method has some advantages compared to general BEM:

(1) The fundamental solutions used in general BEM, given as

$$L^*(u^*) = \delta(x - \xi),$$

where $L^*(\cdot)$ is the adjoint operator to $L(\cdot)$ and $\delta(x-\xi)$ is the Dirac delta function, are usually complex and difficult to obtain. In contrast, the proposed meshless method requires the fundamental solution of the standard Laplacian operator only, even in complex problems.

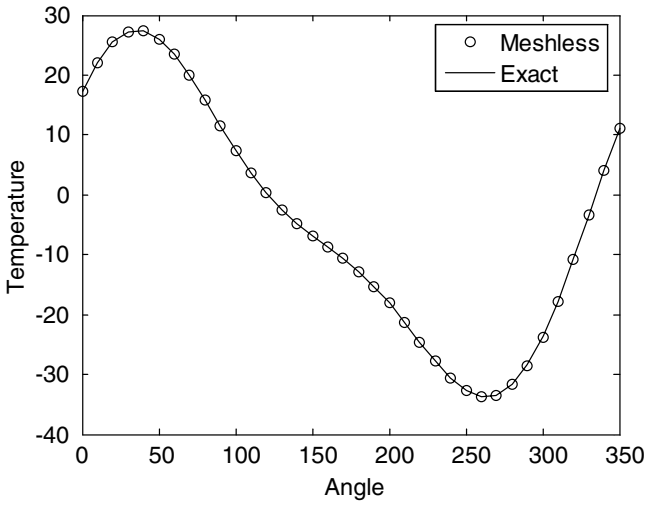


**Fig. 23.** Comparison of temperature between numerical and exact results on the ellipse which has a semimajor axis of length 1.25 and a semiminor axis of length 0.75

(2) No boundary element is required in the method, and thus the general singular integral is avoided.

(3) There are no extra integral equations required to compute the internal properties.

(4) The computational process is relatively simple and the theoretical basis is simple.

Finally, numerical results show clearly that the method presented can achieve very high accuracy with a relatively small number of collocation points, and the local RBF used to interpolate the fictitious body-force terms shows itself to be superior.

## References


1. **Nowak, A.J.; Brebbia, C.A.:** The multiple-reciprocity method. A new approach for transforming BEM domain integrals to the boundary. Eng Anal Bound Elem 6(3) 164–167 (1989)
2. **Nowak, A.J.; Brebbia, C.A.:** Numerical verification of the multiple reciprocity method for linear potential problems with body forces. Eng Anal Bound Elem 10 259–266 (1992)
3. **Nardini, D.; Brebbia, C.A.:** A new approach to free vibration analysis using boundary elements. In: Brebbia, C.A.: (ed) Boundary element methods in engineering proceedings. 4th International Seminar, Southampton. Springer, Berlin Heidelberg New York 1982 312–326
4. **Nowak, A.J.; Partridge, P.W.:** Comparison of the dual reciprocity and the multiple reciprocity methods. Eng Anal Bound Elem 10 155–160 (1992)
5. **Katsikadelis, J.T.:** The analog equation method–a powerful BEM–based solution technique for solving linear and nonlinear engineering problems. In: Brebbia, C.A.: (ed) Boundary element method XVI. CLM Publications, Southampton (1994) pp. 167
6. **Sun, H.C.; Zhang, L.Z.:** Nonsingularity boundary element methods (in Chinese). Dalian University of Technology Press, Dalian (1999)
7. **Sun, H.C.; Yao, W.A.:** Virtual boundary element-linear complementary equations for solving the elastic obstacle problems of thin plate. Finite Elem Anal Des 27 153–161 (1997)
8. **Golberg, M.A.; Chen, C.S.:** The method of fundamental solutions for potential, Helmholtz and diffusion problems. In: Golberg, M.A.: (ed) Boundary integral methods – numerical and mathematical aspects. Computational Mechanics Publications. pp. 103–176 (1998)
9. **Chen, W.; Tanaka, M.; Meshless, A.:** Integration-free and boundary-only RBF technique. Comput Math Appl 43 379–391 (2002)
10. **Chen, W.; Hon, Y.C.:** Numerical investigation on convergence of boundary knot method in the analysis of homogeneous Helmholtz, modified Helmholtz, and convection–diffusion problems. Comput Methods Appl Mech Eng 192 1859–1875 (2003)
11. **Chen, W.:** Meshfree boundary particle method applied to Helmholtz problems. Eng Anal Bound Elem 26 577–581 (2002)
12. **Chen, W.:** High-order fundamental and general solutions of convection–diffusion equation and their applications with boundary particle method. Eng Anal Bound Elem 26 571–575 (2002)
13. **Chang, Y.P.; Kang, C.S.; Chen, D.J.:** The use of fundamental Green's functions for the solution of heat conduction in anisotropic media. Int J Heat Mass Transfer 16 1905–1918 (1973)
14. **Partridge, P.W.:** Approximation functions in the dual reciprocity method. Int J Bound Elem Commun 8 1–4 (1997)
15. **Zhang, Y.; Zhu, S.:** On the choice of interpolation functions used in the dual-reciprocity boundary-element method. Eng Anal Bound Elem 13 387–396 (1994)
16. **Golberg, M.A.; Chen, C.S.; Bowman, H.:** Some recent results and proposals for the use of radial basis functions in the BEM. Eng Anal Bound Elem 23 285–296 (1999)

17. **Yamada, P.W.; Wrobel, L.C.; Power, H.:** On the convergence of the dual reciprocity method. Eng Anal Bound Elem 13 291–298 (1994)
18. **Mitic, P.; Rashed, Y.F.:** Convergence and stability of the method of meshless fundamental solutions using an array of randomly distributed sources. Eng Analy Bound Elem 28 143–153 (2004)
19. **Kassab, A.J.; Divo, E.:** A generalized boundary integral equation for isotropic heat conduction with spatially varying thermal conductivity. Eng Analy Bound Elem 18 273–286 (1996)
20. **Divo, E.; Kassab, A.J.:** Generalized boundary integral equation for heat conduction in non-homogeneous media: recent developments on the sifting property. Eng Anal Bound Elem 22 221–234 (1998)
21. **Mera, N.S.; Elliott, L.; Ingham, D.B.; Lesnic, D.:** A comparison of boundary element method formulations for steady state anisotropic heat conduction problems. Eng Analy Bound Elem 25 115–128 (2001)